Mechanical and wear behaviour of hot-pressed 304 stainless steel matrix composites containing TiB2 particles

Sahoo, S.; Jha, B.B.; Mahata, T.; Sharma, J.; Murthy, T.S.R.C.; Mandal, A.

DOI:
10.1007/s12666-019-01588-1

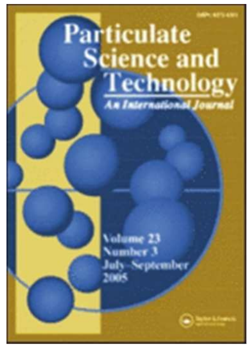

Mechanical and wear behavior of hot pressed 304 stainless steel matrix composites containing TiB2 particles

Journal:	*Particulate Science and Technology*
Manuscript ID	UPST-2018-1788
Manuscript Type:	Original Article
Date Submitted by the Author:	31-Jul-2018
Complete List of Authors:	Sahoo, Silani; Institute of Minerals and Materials Technology CSIR, Advanced Materials Technology Department Jha, Bharat; CSIR-Central Glass & Ceramic Research Institute, Business Development & Standardisation Division Mahata, Tarasankar; Bhabha Atomic Research Centre, Powder Metallurgy Division Sharma, Jyothi; Bhabha Atomic Research Centre, Powder Metallurgy Division Murthy, Tammana; Bhabha Atomic Research Centre, Materials Processing and Corrosion Engineering Division Mandal, Animesh; Indian Institute of Technology Bhubaneswar - Toshali Campus, School of Minerals, Metallurgical and Materials Engineering
Keywords:	304 stainless steel, TiB2, hot pressing, microstructure, mechanical properties < ceramics, wear

Mechanical and wear behavior of hot pressed 304 stainless steel matrix composites containing TiB_2 particles

Silani Sahoo [1*], Bharat B Jha [2], Tarasankar Mahata [3], Jyothi Sharma [3], Tammana SRCh Murthy[4] and Animesh Mandal [5]

[1] Advanced Materials Technology Department, CSIR-Institute of Minerals and Materials Technology, Bhubaneswar, 751013, Odisha, India
[2] Business Development & Standardisation Division, CSIR-Central Glass & Ceramic Research Institute, Kolkata, 700032, West Bengal, India
[3] Powder Metallurgy Division, Bhabha Atomic Research Centre, Navi Mumbai – 400703 Maharashtra, India
[4] Materials Processing and Corrosion Engineering Division, Bhabha Atomic Research Centre, Mumbai - 400 085, Maharashtra, India
[5] School of Minerals, Metallurgical and Materials Engineering, Indian Institute of Technology Bhubaneswar, Bhubaneswar, 751007, Odisha, India

Abstract

In the present article, mechanical and wear behavior of hot pressed 304 stainless steel matrix composites containing 2 and 4 vol.% TiB_2 particles were investigated. A density of over 92% was achieved at optimum hot pressing temperature and volume fraction of TiB_2 particles. Microhardness and yield strength of the composites was found to be improved remarkably as compared to their unreinforced counterpart. The enhancement of mechanical properties of the composites was discussed in light of their microstructural aspects and different possible strengthening mechanism models. Taylor strengthening was found to be dominant strengthening mechanism as compared to Orowan strengthening and load bearing effect. Dry sliding wear behavior was also investigated under load of 35 N at sliding speed 0.3 m/s. The wear resistance of the composites were found to be improved owing to uniform distribution of hard TiB_2 particles. Based on our findings, it was concluded that processing parameters and amount of TiB_2 have significant influence on mechanical and wear behavior of steel matrix composites.

Keywords: 304 stainless steel; TiB_2; hot pressing; microstructure; mechanical properties; wear

***Corresponding author:** Email: silanisahoo@immt.res.in

1. Introduction

Metal matrix composites (MMCs) are tailored to possess properties not exhibited either by matrix or the reinforcement. The metallic matrix may be aluminium, copper, magnesium, titanium, zinc and their alloys (Akhtar 2014; Rana and Liu 2014; Springer et al. 2015). Improvement in the properties of MMCs such as hardness, wear and corrosion resistance, specific modulus, ductility and fracture toughness represents a major challenge due to its dependence on interplay of several processing and microstructural parameters. These microstructural parameters are influenced by volume fraction of ceramic reinforcements, shape and size of reinforcements, interface between ceramic reinforcement and matrix material, composition of matrix, defects, cracks and distribution of reinforcements in the matrix (Chen et al. 2016; Baron et al. 2016). In recent years, iron based alloys and steels have also been widely researched as matrix owing to their low cost, availability and adequate mechanical properties. However, austenitic stainless steels are susceptible to many common forms of wear and friction damage due to their low hardness which limits their application in tribological environment (Sulima et al.2016). A promising pathway to overcome this deficiency is the introduction of suitable hard ceramic particles. Steel matrix composites can be more viable in their application by improving the properties and finding more economical synthesis techniques. Thus the requirement of low cost along with enhanced toughness and wear resistance has led to significant interest in development of ceramic reinforced steel matrix composites. However, in order to achieve the desired properties, proper choice of sintering condition, nature of reinforcement, size and content of reinforcements are very crucial. Literature shows an increase in wear resistance of MMCs with increase in the volume fraction of reinforcement (Moazami-Goudarzi and Akhlaghi 2016; Jin et al.2017; Chi et al.2015). Ease of processing and affordability could provide a greater scope for potential application of steel matrix composites, and thus various types of reinforcements are being incorporated by the researcher to realise this objective.

In this direction, TiB_2 as reinforcement in steel matrix has received lot of attention recently. This can be attributed to unique properties of TiB_2 such as low density (4.5 g/cc), high melting point (3225 ºC), high elastic modulus (430 GPa), high hardness (~32 GPa), good abrasion resistance and good wettability and stability in steel matrix (Sulima et al.2011; Wang et al.2013). These excellent properties make it attractive for many high performance structural applications such as cutting tools, crucibles, wear resistance and corrosion resistance parts. Although, several methods for fabrication of steel matrix composites are known (Yang et al.2009; Zhang et al.2007; Pagounis and Lindroos 1998; Lepakova et al.2004), homogeneous distribution of reinforcement still remains a challenge and efforts needed to address this issue. Powder processing route is considered as economically viable and attractive route for the synthesis of particle reinforced MMCs owing to less reactivity between matrix and reinforcement. Also, powder metallurgy route allows for wide range of reinforcement with higher content (Bains et al.2016). Although a variety of powder metallurgy based approaches have been developed to synthesize these types of composites to obtain excellent combination of the properties, little research has been done to understand the strengthening mechanisms in TiB_2 reinforced steel matrix composites (Wang et al.2006; Sulima et al.2014; Tjong and Lau 2000). Sulima et al. (2014) reported a minimum friction coefficient (0.32) and specific wear rate ($208x10^{-6}$) for composite containing 8 vol.% TiB_2 and sintered at 1300 ºC by spark plasma method. In another work, similar enhancement of wear resistance was observed in AISI 316L stainless steel reinforced with 8 vol.% TiB_2 particles prepared by high pressure-high temperature (HP-HT) method (Sulima et al. 2014). Tjong and Lau .(1999) reported improvement of the wear resistance of AISI 304 stainless steel reinforced with 20 vol.% TiB_2 particles synthesized by hot isostatic pressing (HIP).

They also observed decrease in volumetric wear of the composite with increasing applied normal loads or with sliding velocity.

It is apparent that despite extensive research on synthesis by HT-HP, HIPing, SPS, attempts to synthesize steel matrix by hot pressing method is not reported. Hot pressing method is a cost effective powder metallurgy route along with extensive applications in industries. In addition, this method ensures uniform distribution of particles in the matrix and thus contributing to the enhancement in the strength. In light of these facts, we speculate fabrication of steel matrix composite by hot pressing route would not only be economical as compared to existing powder metallurgy routes but also enhance its potential in many advanced applications. Therefore, the current work is intended to study the influence of TiB_2 and hot pressing sintering temperature on mechanical and wear properties of the hot pressed composites. In addition, the possible strengthening mechanisms operating for enhancement in strength of these composites are also be explored.

2. Materials and methods

In the present investigation, commercially available AISI 304 Stainless Steel (AISI 304 SS) powder with an average particle size of 28 μm supplied by Nanoshell, India was used as the matrix and the chemical composition is shown in Table 1. TiB_2 powders with an average particle size of 2 μm was used as reinforcement (Subramanian et al.2007). To achieve homogeneous mixing, steel powder and TiB_2 powder (2 vol.% and 4 vol.%) were mixed in a high energy ball mill (Model: PM-400) for 2 hours. Then the resulting mixed powders were loaded in a graphite die having inner diameter 30 mm. Thereafter, consolidation of mixed powders were done by uniaxial vacuum hot pressing (Vacuum Tech Pvt. Ltd., India) at 1000 ºC and 1100 ºC with heating rate of 25 ^{0}C/min for 15 minutes at 48 MPa pressure. Finally, disc shaped compacts with diameter 30 mm and thickness 3 mm were sectioned.

The densities of the hot pressed compacts were estimated by Archimedes water immersion method. Relative density was evaluated from theoretical absolute density and experimentally observed density. The theoretical densities of the resultant composites were calculated following the rule of mixtures, considering the theoretical densities for steel and TiB_2 as 7.9 gm/cm^3 and 4.5 gm/cm^3 respectively (Sulima et al. 2014). For metallographic study, the hot pressed compacts were sectioned and polished as per standard procedure. Microstructural assessment of the samples was then conducted using Scanning Electron Microscope (SEM) (Model: Zeiss EVO18) equipped with Energy Dispersive X-ray spectroscopy (EDS) for chemical microanalysis. Distribution of elements in the matrix was analysed by conducting EDX attached with SEM.

Vickers indentation tests (HV0.1) was carried out on polished surface of the hot pressed samples using a 136 ^{0} Vicker diamond pyramid indenter under a load of 0.98 N (100 gf) at room temperature. Compression test was performed in order to investigate the behavior of the synthesized composites with different volume fractions of TiB_2 under the influence of compressive load. The compression test samples were sectioned from hot pressed compact in cylindrical shape having a diameter of 2.5 mm and height of 5 mm as per ASTM standard. The compression test was carried out by using a servo hydraulic universal testing machine (INSTRON 8801) with a constant strain rate of 1 mm/min. at room temperature. A photograph of testing machine and schematic picture of compressive sample is shown in Figure 1a and b. Four compression tests were conducted for each sample for analysing the results and compressive yield strength was reported by taking the average of these four results. Wear test was conducted in order to study the tribological performance of the synthesized composites as a function of TiB_2 content. Dry sliding wear test was performed by block-on-disc method using multiple tribo Tester (Model: TR-25, DUCOM, Bangalore) on prepared composite specimens at sliding speed 0.3 m/s with normal load of 35 N. The counter wheel material was made of EN 31 steel coated with titanium aluminium nitride (TiAlN). A block of size 9 mm x 6.5 mm x 3 mm machined from the synthesized composite for wear testing as per ASTM G 77-98 standard. Before testing, the flat surface of the specimens was polished to achieve uniform surface finish. Wear tests were carried out at room temperature without lubrication for 30 min. Wear of specimen in terms of wear depth and coefficient of friction was recorded automatically during the tests.

3. Results and discussion

3.1 Microstructure

Figure 2 shows the SEM micrograph of hot pressed unreinforced steel matrix along with total area EDX analysis. EDX results confirmed the presence of Fe, Cr, Ni as main elements without presence of any foreign elements. Figure 3 gives the SEM micrograph of composite with 2 vol.% TiB_2 with EDX results at the indicated points. As shown in Figure 3, point 1 presents TiB_2 (light grey colour) and point 2 presents matrix phase which can be supported by corresponding EDX results. Point 1 consists of Ti and B while point 2 consists of Fe, Cr, Ni etc. SEM micrograph also reveals relatively uniform distribution of TiB_2 along the grain boundary which contributes to enhanced mechanical properties. Figure 4 presents the SEM micrograph of composite with 4vol.% TiB_2 along with corresponding EDX mapping. The map shows the elemental distribution of Ti and B along with the parent matrix elements. The average reinforcement particle size was found to be in the range of 0.7-0.8 µm. Clustering of particles are also observed in some location in composite containing 4 vol.% TiB_2 (as shown in Figure 4 which is quite expected due to increase in volume fraction of fine reinforcement particles(Leszczyńska-Madej et al.2017).

3.2 Density

The relative density of the investigated hot pressed samples is shown in Figure 5. The relative density of resultant composites range from 87 - 92% of theoretical density. The inconsistency between theoretical and experimental values of density indicates presence of porosity. The density of composite decreases from 7.10 to 6.91 when TiB_2 content increases from 2 vol.% to 4 vol.% due to low density of TiB_2. Again, a significant difference in relative density can be observed in the specimen pressed at 1000 ºC and 1100 ºC with same TiB_2 content. This can be attributed to influence of temperature on solid state diffusion mechanism thereby increasing sinterabilty and hence densification. Further, the more uniform distribution of TiB_2 particles in the matrix at high temperature as evident from microstructure can attenuate the pinning effect of second phase particles and accordingly increase densification (Pagounis and Lindroos 1998). Therefore, there is a need to optimize hot pressing parameters to maximize densification.

3.3 Hardness

The results of microhardness tests of composites synthesized by hot pressing are shown in Figure 6. It can be observed that hardness of steel matrix composite shows an increasing trend with increasing amount of TiB_2 particles. This is due to presence of hard TiB_2 particles in the matrix that results in constraint to plastic deformation of soft matrix during indentation. For particle reinforced MMC, increasing the volume content of reinforcements results in a low interparticle spacing and consequently leading to higher stresses for the passage of dislocations through the hard ceramic phase for a given reinforcement particle size (Sulima et al. 2014)). From Figure 6, it is evident that the hardness increases with increasing processing temperature irrespective of TiB_2 content. This is due to higher densification of composite at higher temperature and uniform distribution of particles along the grain boundary as evident from the microstructure resulting in increased hardness. Sulima et al.(2014) reported similar type of observation for steel matrix composites sintered by spark plasma process. Among the samples investigated in the current study, steel matrix composite reinforced with 4 vol.% TiB_2 hot pressed at 1100 ºC exhibited highest hardness value as compared to other prepared samples. It is interesting to note that amount of reinforcement phase determines the hardness of composites in the present work rather than the porosity in the microstructure. This observation could be attributed to high hardness value of TiB_2 and good interface bonding between the particle and matrix. Further it is well known that introduction of hard ceramic particles increases the strain energy by generation of dislocation due to difference in thermal expansion coefficient between matrix and reinforcement thereby resulting high hardness(Leszczyńska-Madej et al.2017).

3.4 Compressive properties

Typical compression behavior of hot pressed 304- TiB_2 composites is shown in Figure 7. The compression strength of the composites are higher than unreinforced steel indicating positive effect of TiB_2 reinforcement on the mechanical properties of steel. The compressive strength increase at the expense of ductility. This finding can be ascribed to dominating role of TiB_2 for enhancement of compressive strength over deterioration effect of increased porosity. The compressive yield strength of hot pressed steel matrix without reinforcement is in the range of 945 - 1227 MPa. The compressive yield strength of the composites sintered at 1000 ºC with 2 vol.% of TiB_2 and 4 vol.% of TiB_2 content are 1124 MPa and 1279 MPa respectively. However, the plastic deformation of the hotpressed samples decreases from 23% for the unreinforced steel to 18% for the composites with 2 vol.% of TiB_2 and to 15% for the composites with 4 vol.% of TiB_2. Lowering of ductility is due to presence of TiB_2 that prevents the plastic deformation and blocks the dislocation motion. Comparing Figure 7a and b, an increase in strength of the composites can be observed with increase in processing temperature. The ultimate compressive yield strength of hot pressed steel matrix without reinforcement increases from 945 MPa (sintered at 1000 ºC) to 1227 MPa (sintered at 1100 ºC). Therefore it is also noteworthy that samples pressed at 1100 ºC exhibited notably high strength as compared to samples hot pressed at 1000 ºC which can be attributed to their low porosity and adequate bonding between the particles. Based on the results, it is clear that the compressive yield strength increased with increasing processing temperature indicating significant relationship between processing temperature and mechanical properties. It is also confirmed that strength of the reinforced steel matrix has not deteriorated despite the presence of porosity.

3.4.1. Strengthening mechanisms

Several mechanisms and models have been recommended in order to provide more insight towards the enhancement of strength of metal matrix composites. Such as (a) Load transfer from the matrix to the reinforcement particle at the interface (shear lag model) (b) Increased dislocation densities produced on cooling due to large difference in coefficient of thermal expansion (CTE) of the matrix and that of the reinforcement particles (Taylor strengthening) (c) Orowan strengthening due to artificially reduction in inter particle spacing (d) Work hardening due to presence of hard ceramic particles (Asl and Kakroudi 2015). All the above said mechanisms are expected to be suitable for steel matrix composites synthesized in the present work.

First, the relation between dislocation density and strengthening has long been established by many researchers (Chelliah et al.2017).When a metal matrix composite is subjected to temperature change, dislocations are generated in the vicinity of ceramic reinforcement due to difference in coefficient of thermal expansion (CTE) between matrix and reinforcement so as to reduce the stored energy. In the present work, all the fabricated samples are imposed to temperature difference of 975 ºC for processed at 1000 ºC and 1075 ºC for processed at 1100 ºC. Again, the difference in CTE between steel matrix and TiB_2 particle is $10x10^{-6}$/K which can lead to generation of geometrically necessary dislocations in order to accommodate this thermal mismatch. The increment in the yield strength due to generation of dislocation owing to relaxation of thermal mismatch or Taylor strengthening can be expressed as (Zhang and Chen 2006):

$$\Delta\sigma_{CTE} = \beta G_m b \sqrt{\frac{12\Delta\alpha\Delta T V_p}{b d_p (1-V_p)}} \quad (1)$$

Where β is strengthening coefficient, G_m is shear modulus of the matrix, b is Burgers vector, $\Delta\alpha$ is the difference of CTE between steel matrix and TiB_2 particles, ΔT is the difference between the processing and test temperature, V_p and d_p present the volume fraction and average particle size of TiB_2 reinforcements.

Another aspect that can contribute to the enhancement of strength is Orowan strengthening from dispersoids present in the matrix. The Orowan strengthening model describes improvements in strength in the matrix material due to formation of dislocation loops around the particles (Zhang and Chen 2006). It is generally believed that the Orowan strengthening mechanism is not significant for metal matrix composites reinforced with a particle size greater than 5 micron (Xiao et al.2018). In the present work, average particle size of the reinforcement is in submicron range (0.7-0.8 μm) indicating Orowan strengthening can contribute slightly to the improvement of yield strength of composites (Nie et al.2017). The contribution of Orowan strengthening in MMC increases with increase in volume fraction of reinforcement particles and decrease in interparticle spacing between dispersoids which impedes the movement of dislocation (Chelliah et al.2017).Increment of yield strength due to Orowan strengthening can be described by the following expression below: (Nie et al.2017).

$$\Delta\sigma_{orowan} = \frac{0.13 G_m b}{d_p\left[(1/2V_p)^{\frac{1}{3}}-1\right]} \ln\left(\frac{d_p}{2b}\right) \quad (2)$$

In addition, the load transfer strengthening mechanism can be used to explain the improvement of yield strength of the composites due to load bearing effect of hard ceramic phase. It is reported that the good interfacial bonding between dispersed particles and matrix contributes to better transfer of the applied load to the reinforcement. The enhancement of strength due to load transfer effect can be described by (Dai et al.2001)

$$\Delta\sigma_{Load} = 0.5V_p\sigma_m \quad (3)$$

Where σ_m is the yield strength of matrix and V_p is the volume fraction of TiB_2 particles.

The parameters and properties used for calculating the improvement in yield strength of the composites by various strengthening mechanisms are listed in Table 2.

Based on above governing equations for different strengthening mechanisms, the enhancement of yield strength of the composites with different content of TiB_2 and processing temperature was calculated and shown in Figure 8. It can be seen that contribution due to thermal mismatch strengthening mechanism plays a significant role towards enhancement of strength as compared to other strengthening mechanisms. The predominance effect of thermal mismatch strengthening can be attributed to large difference in temperature and coefficient of thermal expansion that increases the magnitude of thermal strain ($\Delta\varepsilon_T = \Delta\alpha\Delta T$) and density of geometric dislocation. In Figure 8a and b, dislocation strengthening in the composites show an increasing trend with increase in TiB_2 content and processing temperature. Further, it can be noticed that load transfer strengthening contributed slightly due to low volume fraction of TiB_2 in the current work. The observed results also reveal the relative contribution of Orowan strengthening in composite with 4 vol.% TiB_2 is increased by 1.45 times as compared to composite with 2 vol.% TiB_2. This observation can be attributed to decrease in interparticle distance with increase in TiB_2 resulting in enhanced pinning effect and more restriction of plastic flow of the matrix and improved strength. However based on the above results, we can conclude that Taylor strengthening due to thermal mismatch plays as most dominating strengthening mechanism compared to others.

Several numerical models are available for estimation of theoretical yield strength of particle reinforced MMCs. Among these methods, modified Zhang and Chen model and summation models are commonly used to predict the yield strength of particle reinforced MMCs (Zhang Z and Chen 2006; Xiao et al.2018; Frost and Ashby1982). Zhang and Chen model is based on the assumption of interdependent relationship between individual strengthening mechanisms. This model includes the effect of Orowan strengthening, thermal mismatch strengthening and load bearing. The theoretical increase in yield strength by this model can be expressed as follows:

$$\Delta\sigma_{ZC} = \left(1 + 0.5V_p\right)\left[\sigma_{ym} + \Delta\sigma_{Orowan} + \Delta\sigma_{Taylor} + \left(\frac{\Delta\sigma_{Orowan}\Delta\sigma_{Taylor}}{\sigma_{ym}}\right)\right] \quad (4)$$

On the other hand, summation model considers all the strengthening contribution acting individually on the materials. The theoretical increase in yield strength by this model can be described by:

$$\Delta\sigma_S = \sigma_{ym} + \Delta\sigma_{Orowan} + \Delta\sigma_{Taylor} + \Delta\sigma_{Load} \quad (5)$$

Figure 9 presents a comparison between the experimental values of yield strength of composites and theoretical values estimated by Zhang and Chen model and summation model. Figure 9a and b also confirms the improvement of strength with increase in TiB_2 content and processing temperature. The estimated yield strength from model approximates the experimental values. The experimental yield strength is higher than the model values indicating contribution of other strengthening mechanisms. Thus it is clearly evident that existence of particle and particle size distribution should be considered for enhancement of strength.

3.5 Elastic modulus

Elastic modulus of particle reinforced composites can be calculated using the simple rule-of mixtures (ROM) (Kim et al.2013).

Under iso-strain condition, $E_C = E_pV_p + E_mV_m$ (6)

Under iso-stress condition, $E_C = \frac{E_pE_m}{E_pV_m+E_mV_p}$ (7)

Where V_p stands for volume percentage of TiB_2 particulate, V_m stands for the volume fraction of matrix, E_p is the elastic modulus of TiB_2 particulate, and E_m is the elastic modulus of matrix.

However, effective modulus of particulate composites can be evaluated by Halpin–Tsai (HT) model (Reddy and Zitoun 2011) that takes into account the aspect ratio of the reinforcements in addition to the volume fraction and elastic modulus of the reinforcements and matrix and is expressed as

$$E_c = \frac{E_m(1+2sqV_p)}{1-qV_p} \quad (8)$$

where E_c and E_m present the Young's moduli of the composite and the matrix respectively, s is the aspect ratio of the reinforcement, V_p is the volume fraction, and q is a geometrical parameter that can be written as

$$q = \frac{\left(\frac{E_p}{E_m}\right)-1}{\left(\frac{E_p}{E_m}\right)+2s} \quad (9)$$

Substituting the values of elastic modulus of steel as 193 GPa and elastic modulus of TiB_2 as 430 GPa (Sulima et al.2011) in equations (6) to (9), elastic modulus for composites with different content of TiB_2 are calculated. Comparative analysis between estimated values of elastic modulus and the experimental value is presented in Figure 10. The experimental values matches well with the values estimated by HT model and ROM. The experimental results indicate a significant improvement in elastic modulus of the composite with 4 vol.%. TiB_2 particles. This remarkable improvement in the elastic modulus of the composites can be mainly attributed to high elastic modulus of reinforcing TiB_2 particle and homogeneous distribution of reinforcement particles in the matrix. In addition, increase in interfacial area with increase in volume fraction of reinforcement particles enhances the stress transfer from plastically deforming ductile metal matrix to hard, brittle reinforcing particles. It is also evident that experimental value of elastic modulus of unreinforced steel is lower than the theoretical value which can be ascribed to lower relative density of the sample.

3.6 Wear properties

Wear behavior of material can be expressed by depth of wear that indicates removal of material from the surface. Figure 11 shows wear depth curves of unreinforced steel matrix and composite reinforced with 2 vol.%, 4 vol.% TiB_2 sintered at 1000 ºC and 1100 ºC. It is apparent that depth of wear approaches a steady state wear regime within few seconds of commencement of the test. The depth of wear of composites is low as compared to unreinforced steel. Also, depth of wear decreases with increase in volume percentage of TiB_2 indicating enhanced wear performance. This enhancement can be attributed to increased hardness and strength due to presence of higher amount of hard TiB_2 particles. The higher amount of TiB_2 particles increases the load carrying capacity and resistance to plastic deformation by impeding dislocation motion. It has been reported that particles are the most effective in improving the wear resistance of MMCs (Moazami-Goudarzi and Akhlaghi 2016; Jin et al.2017; Chi et al.2015; Jin et al.2017). It is well known that hardness of MMCs increases with increase in amount of reinforcement particles thereby significantly influencing the wear resistance by decreasing in real area of wear surface. Reports of earlier research on wear behavior of particle reinforced MMCs demonstrated the dependence of wear resistance on hardness as well as mean free path between the reinforced particles. In general, wear resistance is proportional to H/ λ (Jin et al.2017) where H represents hardness and λ represents mean free path. Literature suggests that interparticle spacing plays an important role in wear resistance of composites. It depends on the reinforcement particle size d and the volume fraction f by the expression as

$$\lambda \propto d/\sqrt{f} \qquad (10)$$

This expression predicts shorter mean free path for higher volume fraction of reinforcement particles. According to the present results, wear resistance of the 4 vol.% TiB_2/steel composite is higher as compared to 2 vol.%TiB_2/steel composites. Based on the above results, it is reasonable to assume that wear resistance of the present composites is improved due to decrease in λ owing to increase in TiB_2 content. Decrease in λ results in reduction of indentation depth of soft abrasive particles with almost no significant grooves. Similar tendency of increase of wear response and hardness was reported by Tjong and Lau (2000) and Sulima et al. (2014) for TiB_2 reinforced steel MMCs synthesized by powder metallurgy methods. Mahajan et al. (2015) investigated the influence of wettability on the wear behavior of composite. They reported good bonding between matrix and reinforcement ensures improved wear resistance. So observation of steady state wear regime in our results confirm the good bonding between TiB_2 particles and steel matrix. The present results indicate decrease in depth of wear of the samples with increase in hot pressing temperature as shown in Figure 11b. This is quite obvious because increase in sintering temperature in the present case enhances the hardness as compared to composites sintered at lower temperature. This finding is in support of Archard's wear law which suggests an inverse relationship between hardness and wear rate. As far as the wear behavior of composites is concerned, it is influenced by microstructural properties and nature of reinforcement. Composites sintered at higher temperature were accompanied with higher density that leads to lower wear depth due to a reduced amount of loss of adherence of particles. Another suggested reason for enhancement of wear performance is uniform distribution of reinforcement particles in the matrix as evident in the microstructure. Present results are consistent with investigations of Sulima et al.(2014) who reported similar variation of wear behavior with sintering temperature for steel matrix composites containing 4 and 8 vol. % TiB_2 fabricated by SPS process. Hence, it is worth to state that addition of TiB_2 reinforcements are most effective for enhancement of wear performance of steel matrix composites as compared to unreinforced steel.

Figure 12 shows coefficient of friction (COF) of the specimens with test duration at an applied load of 35 N and a sliding speed 0.3 m/s. It is very evident from the Figure 12 that COF values are almost steady with testing time indicating minimal damage due to dominating role of TiB_2 to sliding behavior at this load. It can be seen that variation of coefficient friction has a similar trend as that for depth of wear. The COF decreases with the increase of TiB_2 content. Average value of COF of the unreinforced steel sintered at 1000 ºC is in the range of 0.37-0.51 whereas that of composites reinforced with 2 vol.% and 4 vol.% TiB_2 are in the range of 0.29-0.40 and 0.28-0.31 respectively. The influence of TiB_2 on tribological properties of composites can be clearly observed from the graph. This observed variation in COF depending upon reinforcement content can be explained by degree of plastic deformation. The simplified theory of friction proposed by Bowdon and Tabor is given by the following relation (Chelliah et al.2016):

$$\mu = \tau_i / 2.8Y \tag{11}$$

where μ stand for coefficient of friction, τ_i stands for shear strength and Y represents flow pressure or hardness of the material. This equation represents an inverse relationship between hardness and coefficient of friction. Materials exhibits lower μ with higher hardness due to minimal degree of plastic deformation. In the present investigation, it is apparent that composites with 4 vol.% TiB_2 results in higher hardness as compared to other samples. Hence, it can be concluded that higher amount of TiB_2 provide more protection to steel matrix during sliding by inhibiting plastic deformation and delaying material removal from the surface. Furthermore, the results revealed the dependence of the friction coefficient of the composites on the sintering temperature with the same content of TiB_2 particles as shown in Figure 12b. It is interesting to note that application of higher sintering temperature play a remarkable role in improving the wear behavior of sintered composites with the same content of TiB_2. Coefficient of friction values of unreinforced steel decreases from 0.51 to 0.46 with increase in temperature from 1000 ºC to 1100 ºC. The lowest value of the coefficient friction was obtained in composite with 4 vol.% of TiB_2 sintered at 1100 ºC as compared to sintered at 1000 ºC. In the case of composites with 2 vol.% TiB_2, the friction coefficient is 0.40 for sintering temperature of 1000 ºC and reduces gradually to 0.34 at sintering temperature of 1100 ºC. Based on these results, it can be clearly seen that sintering temperature acts as another influential parameter for control of wear performance of composites irrespective of content of TiB_2 particles in the matrix. Higher sintering temperature favours more homogeneous distribution of the fine reinforcements as shown in Figure 4 which results in enhancement of wear resistance due to increase in load bearing capacity by reducing the contact area between specimen and counterpart. Moreover, based on the Archard's equation, wear performance of composites increases with the increased hardness, by increasing the resistance of material to plastic deformation. Similar trend in variation of COF with respect to reinforcement content and sintering temperature have been also reported by other researchers in previous studies (Sulima 2014; Tjong and Lau .1999; Chelliah et al.2016;Sulima et al.2016). Thus it can be concluded that incorporation of TiB_2 particles into steel matrix enhances the wear performance effectively.

4. Conclusions

The following are the major findings based on microstructure, mechanical properties and wear behavior of steel matrix composites reinforced with 2 and 4 vol.% TiB_2 particles synthesized by hot pressing method:

(a) At lower fractions, TiB_2 is uniformly distributed within the steel matrix while few clustering is observed at higher fractions of TiB_2. Optimization of the process parameters is necessary in order to achieve higher densification level.

(b) Steel matrix composites reinforced with TiB_2 particles exhibited high hardness, ultimate compressive strength, elastic modulus and yield strength as compared to their unreinforced counterpart. Hardness of the composites reinforced with 2 vol.% TiB_2 and 4 vol.% TiB_2 was improved by 30% and 42% respectively than that of unreinforced steel sintered at 1100 ºC.

(c) Taylor strengthening caused due to large difference in CTE and temperature change is the major contributor in strengthening these composites. This is followed by Orowan strengthening and load bearing strengthening.

(d) The results of wear tests revealed decrease in depth of wear and COF with increase in the content of TiB_2. The composite with 4 vol.% TiB_2 sintered at 1100 ºC showed the best wear resistance.

Funding

The work was supported by the Board of Research in Nuclear Science (BRNS) of the Department of Atomic Energy (DAE), Government of India (No. 36(2)/14/18/2016- BRNS).

References

Akhtar, F. 2014. Ceramic reinforced high modulus steel composites: processing, microstructure and properties. *Canadian Metallurgical Quarterly* 53: 253-263. doi:10.1179/1879139514Y.0000000135.

Asl, M.S., and M.G. Kakroudi. 2015. A Processing–Microstructure Correlation in ZrB_2–SiC Composites Hot-pressed under a Load of 10 MPa. *Universal Journal of Material Science* 3: 14-21. doi:10.13189/ujms.2015.030103.

Bains, P. S., S.S. Sidhu, and H.S. Payal. 2016. Fabrication and Machining of Metal Matrix Composites: A Review. *Materials and Manufacturing Processes* 31: 553-573. doi:10.1080/10426914.2015.1025976.

Baron, C., H. Springer, and D. Raabe. 2016. Efficient liquid metallurgy synthesis of Fe-TiB_2 high modulus steels via in-situ reduction of titanium oxides. *Materials and Design* 97: 357-363. doi:10.1016/j.matdes.2016.02.076.

Chen, S., Z. Zhao, X. Huang, and L. Zhang. 2016. Interfacial microstructure and mechanical properties of laminated composites of TiB_2-based ceramic and 42CrMo alloy steel. *Material Science and Engineering A* 674: 335–342.doi:10.1016/j.msea.2016.07.106.

Chelliah, N. M., H. Singh, and M K. Surappa. 2017. Microstructural evolution and strengthening behavior in in-situ magnesium matrix composites fabricated by solidification processing. *Materials Chemistry and Physics* 194: 65-76.doi: 10.1016/j.matchemphys.2017.03.025.

Chi. H., L. Jianga, G. Chena, P. Kang, X. Lin, and G.Wu. 2015. Dry sliding friction and wear behavior of (TiB_2+h-BN)/2024Al composites. *Materials and Design* 87; 960–968. doi:10.1016/j.matdes.2015.08.088.

Dai, L.H., Z. Ling and Y.L. Bai. 2001. Size-dependent inelastic behavior of particle-reinforced metal–matrix composites. *Composite Science and Technol*ogy 61:1057-1063.doi: 10.1016/S0266-3538(00)00235-9.

Frost, H.J., and M.F. Ashby.1982. Deformation-Mechanism Maps, The Plasticity and Creep of Metals and Ceramics.1st ed. New york: Pergamon.

Jayakumar, K., J. Mathew, M.A. Joseph, R.K.Suresh, A.K. Shukla, and M.G. Samuel. 2013. Synthesis and Characterization of A356-SiC_p Composite produced through Vacuum Hot Pressing. *Materials and Manufacturing Processes* 28: 991–998. doi:0.1080/10426914.2013.773012.

Jin, C., C.C. Onuoha, Z. N. Farhat, G. J. Kipouros, and K. P. Plucknett. 2017. Reciprocating wear behavior of TiC-stainless steel cermets. *Tribology International* 105: 250–263.doi:10.1016/j.triboint.2016.10.012.

Kim, C.S., Sohn II, Nezafati M, B. Ferguson, B. F. Schultz, Z.B. Gohari Pradeep, K. Rohatgi, and K. Cho. 2013. Prediction models for the yield strength of particle-reinforced unimodal pure magnesium (Mg) metal matrix nanocomposites (MMNCs). *Journal of Material Science* 48: 4191-4204.doi: 10.1007/s10853-013-7232-x.

Lepakova, O. K., L. J. Raskolenko, and Y. M. Maksimov. 2004. Self-propagating high-temperature synthesis of composite material Titanium diboride-Fe. *Journal of Material Science* 39: 3723 - 3732.

Leszczyńska-Madej, B., A. Wąsik, and M. Madej. 2017 Microstructure characterization of SiC reinforced aluminium and Al_4Cu alloy matrix composites. *Archieves of Metallurgy and Materials* 62: 747-755. doi: 10.1515/amm-2017-0112.

Mahajan, G., N. Karve, U. Patil, P. Kuppan, and K. Venkatesan. 2015. Analysis of Microstructure, Hardness and Wear of Al-SiC-TiB_2 Hybrid Metal Matrix Composite. *Indian Journal of Science and Technology* 8: 101-105.doi: 10.17485/ijst/2015/v8iS2/59081.

Moazami-Goudarzi, M., and F. Akhlaghi. 2016.Wear behavior of Al 5252 alloy reinforced with micrometric and nanometric SiC particles. *Tribology International* 102: 28–37. doi.:10.1016/j.triboint.2016.05.013.

Nie, K., K. Deng, X. Wang, and K. Wu. 2017. Characterization and strengthening mechanism of SiC nanoparticles reinforced magnesium matrix composite fabricated by ultrasonic vibration assisted squeeze casting. *Journal of Materials Research* 32: 2609-2620.doi:10.1557/jmr.2017.202.

Pagounis, E., and V. K. Lindroos. 1998. Processing and properties of particulate reinforced steel matrix composites. *Material Science and Engineering A* 246: 221- 234. doi:10.1016/S0921-5093(97)00710-7.

Rana, R. and C. Liu.2014. Effects of ceramic particles and composition on elastic modulus of low density steels for automotive applications. *Canadian Metallurgical Quarterly* 53: 300-316. doi:10.1179/1879139514Y.0000000130.

Reddy, A.C., and E. Zitoun. 2011. Strengthening mechanisms and fracture behavior of 7072Al/Al_2O_3 metal matrix Composites. *International Journal of Engineering Science and Technology* 3: 6090-6100.

Sanaty-Zadeh, A., and P.K. Rohatgi. 2012. Comparison between current models for the strength of particulate-reinforced metal matrix nanocomposites with emphasis on consideration of Hall-Petch effect. *Material Science and Engineering A* 531: 112-118.doi:10.1016/j.msea.2011.10.043.

Springer, H., R. Aparicio Fernandez, M. J. Duarte, A. Kostka, and D. Raabe. 2015. Microstructure refinement for high modulus in-situ metal matrix composite steels via controlled solidification of the system Fe–TiB_2. *Acta Materialia* 96: 47–56.doi:10.1016/j.actamat.2015.06.017.

Subramanian, C., T.S.R.Ch. Murthy, and A.K. Suri.2007.Synthesis and consolidation of titanium diboride. *International Journal of Refractory Metals & Hard Materials* 25:345-350.doi:10.1016/j.ijrmhm.2006.09.003

Sulima, I., L. Jaworska, P. Wyżga, and M. Perek-Nowak. 2011. The influence of reinforcing particles on mechanical and tribological properties and microstructure of the steel- Titanium diboride composites. *Journal of Achievements Materials and Manufacturing Engineering* 48: 52-57.http://www.journalamme.org.

Sulima, I. 2014. Tribological properties of steel/ TiB_2 composites prepared by spark plasma sintering. *Archieves of Metallurgy and Materials* 59: 1263-1268.doi:10.2478/amm-2014-0216.

Sulima, I., L. Jaworska, and P. Figiel. 2014. Influence of processing parameters and different content of Titanium diboride ceramics on the properties of composites sintered by high pressure - high temperature (HP-HT) method. *Archeves of Metallurgy and Materials* 59: 205-209.doi: 10.2478/amm-2014-0033.

Sulima, I., P. Hyjek, and T. Tokarski. 2014. Influence of annealing conditions on the properties and microstructure of steel composites. *Metal Foundry Eng*ineering 40: 33–43.doi:10.7949/mafe.2014.40.1.33.

Sulima, I., S. Boczkal, and L. Jaworska. 2016. SEM and TEM characterization of microstructure of stainless steel composites reinforced with TiB_2. *Material Characterization* 118: 560-569. doi:10.1016/j.matchar.2016.07.005.

Sulima, I., R. Kowalik, and P. Hyjek. 2016. The corrosion and mechanical properties of spark plasma sintered composites reinforced with titanium diboride. *Journal of Alloys Compound* 688: 1195-1205. doi:10.1016/j.jallcom.2016.07.132.

Tjong, S.C., and K.C. Lau. 2000. Abrasion resistance of stainless-steel composites reinforced with hard Titanium diboride particles. *Composite Science and Technol*ogy 60: 1141–1146. doi:10.1016/S0266-3538(00)00008-7.

Tjong, S.C., and K. C. Lau. 1999. Sliding wear of stainless steel matrix composite reinforced with Titanium diboride particles. *Materials Letters* 41: 153–158.doi: 10.1016/S0167-577X(99)00123-8.

Wang, X.H., M.Zhang, and B.S. Du. 2013. Fabrication of Multiple Ceramic Particle Reinforced Iron Matrix Coating by Laser Cladding. *Materials and Manufacturing Processes* 28: 509–513. doi:10.1080/10426914.2012.700154.

Wang, Y., Z. Q. Zhang, H. Y. Wang, B.X. Ma,and Q.C. Jiang. 2006. Effect of Fe content in Fe–Ti–B system on fabricating Titanium diboride particulate locally reinforced steel matrix composites. *Material Science and Engineering A* 422: 339–345. doi: 10.1016/j.msea.2006.02.012

Xiao, P., Y. Gao, C. Yang, Z. Liu, Y. Li, and F. Xu. 2018. Microstructure, mechanical properties and strengthening mechanisms of Mg matrix composites reinforced with in situ nanosized TiB_2 particles. *Material Science and Engineering A* 710: 251–259.doi:10.1016/j.msea.2017.10.107.

Yang, Y.F., H.Y. Wang, RY. Zhao, and Q. C. Jiang. 2009. In Situ TiC/TiB_2 Particulate Locally Reinforced Steel Matrix Composites Fabricated Via the SHS Reaction of Ni–Ti–B_4C System. *International Journal of Applied Ceramic Technology* 6: 437–446.doi: 10.1111/j.1744-7402.2008.02282.x.

Zhang, Z., P. Shen, Y. Wang, and Q. C. Jiang. 2007. Fabrication of TiC and Titanium diboride locally reinforced steel matrix composites using a Fe–Ti–B_4C–C system by an SHS-casting route. *Journal of Material Science* 42: 8350–8356.doi:10.1007/s10853-006-0764-6.

Zhang, Z., and D.L. Chen. 2006. Consideration of Orowan strengthening effect in particulate reinforced metal matrix nanocomposites: a model for predicting their yield strength. *Scripta Materialia* 54: 1321–1326. doi:10.1016/j.scriptamat.2005.12.017.

Figure 1. (a) Image of compressive testing machine (b) Schematic diagram of the specimen.

161x108mm (150 x 150 DPI)

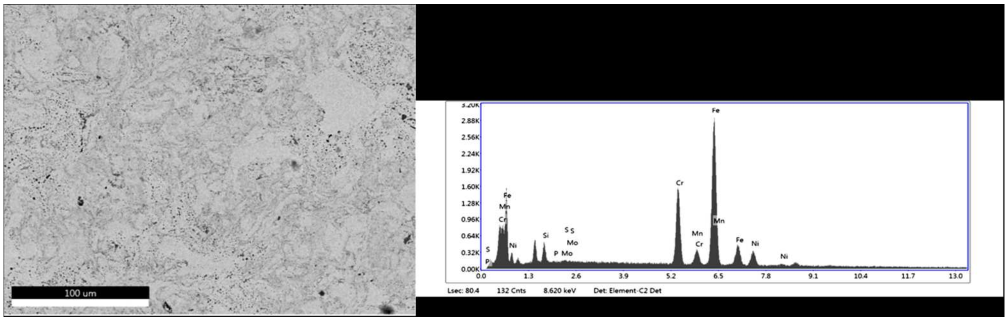

Figure 2. Scanning electron micrograph of unreinforced steel matrix and EDX analysis.

240x75mm (150 x 150 DPI)

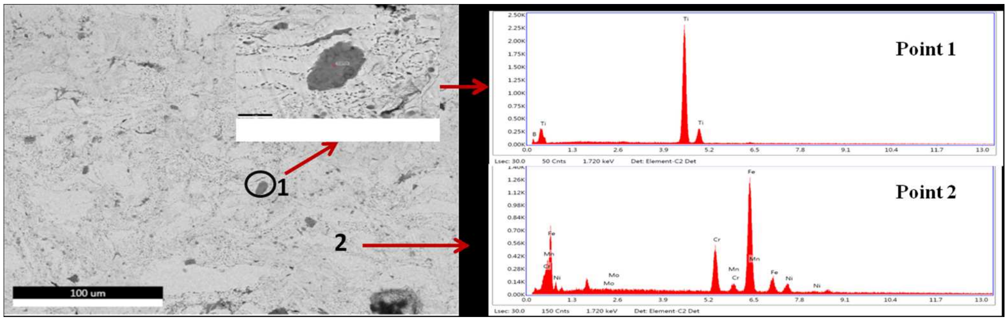

Figure 3. Scanning electron micrograph of composites with 2 vol.% TiB2 along with EDX of indicated points 1 and point 2.

240x75mm (150 x 150 DPI)

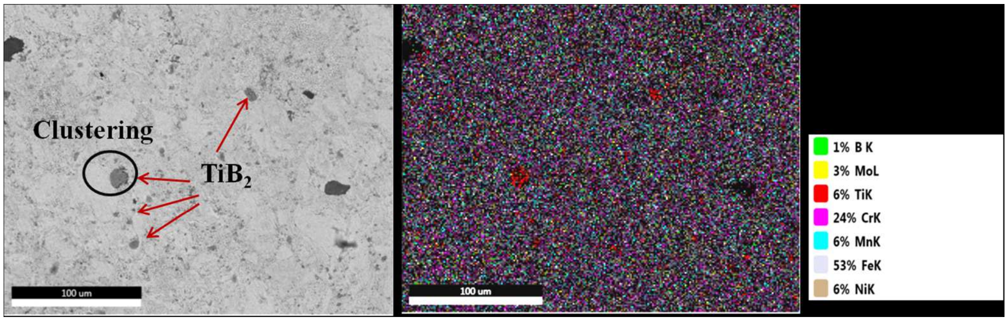

Figure 4. Scanning electron micrograph of composites with 4 vol.% TiB2 along with EDX mapping.

240x75mm (150 x 150 DPI)

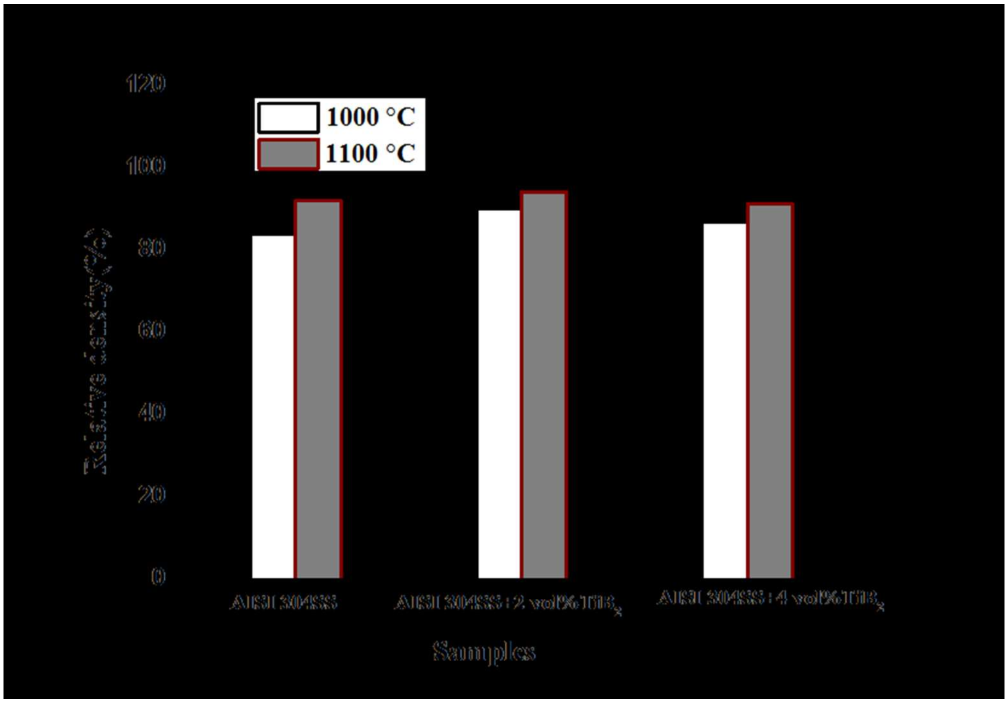

Figure 5. Variation of relative density with the volume percentage of TiB2.

140x97mm (150 x 150 DPI)

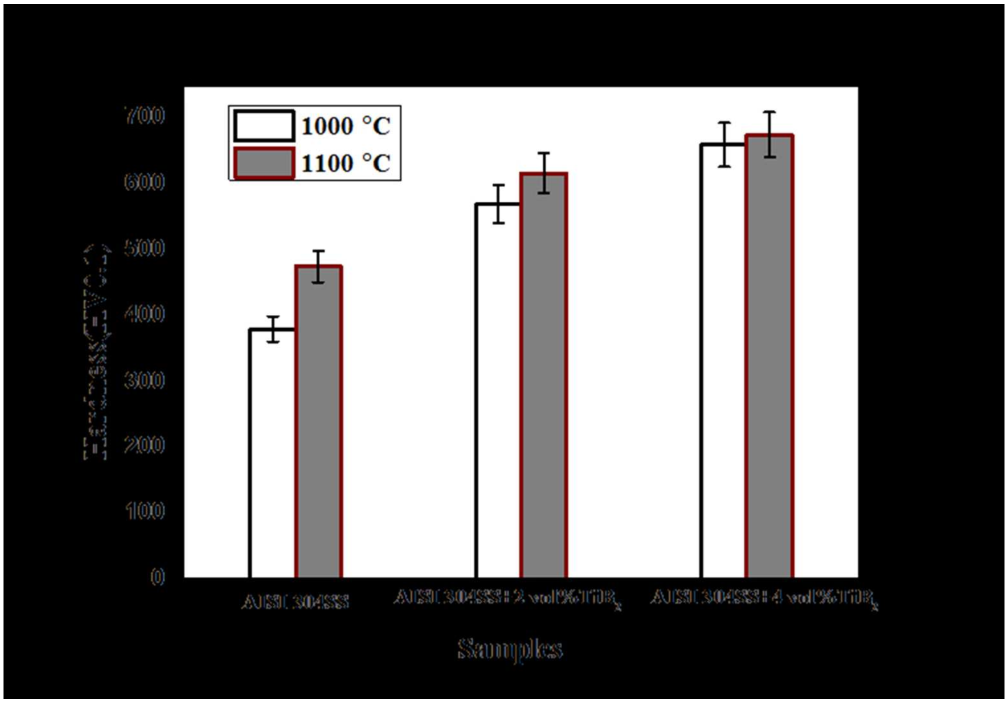

Figure 6. Variation of microhardness with the volume percentage of TiB2.

128x88mm (150 x 150 DPI)

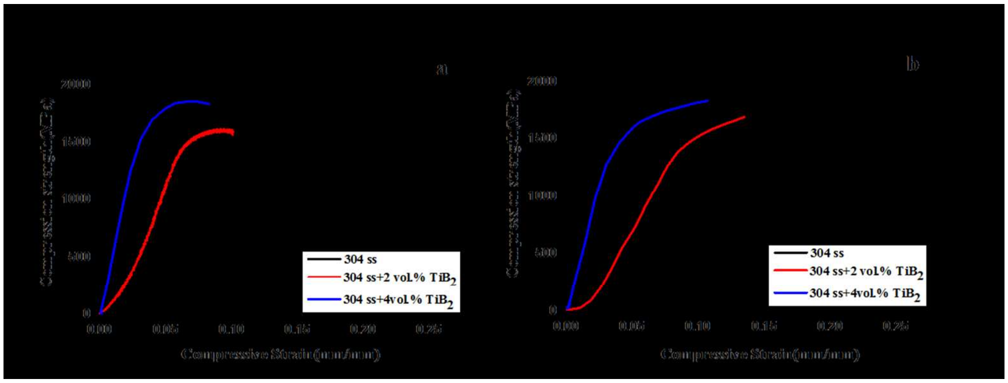

Figure 7. Variation of compression strength of the synthesized composites sintered at (a) 1000 ºC and (b) 1100 ºC

216x81mm (150 x 150 DPI)

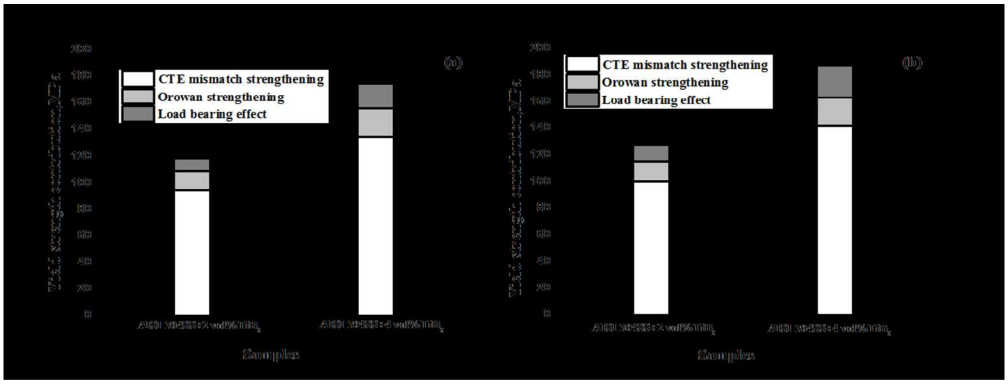

Figure 8. Influence of various strengthening mechanisms in composites sintered at (a) 1000 ºC and (b) 1100 ºC.

214x80mm (150 x 150 DPI)

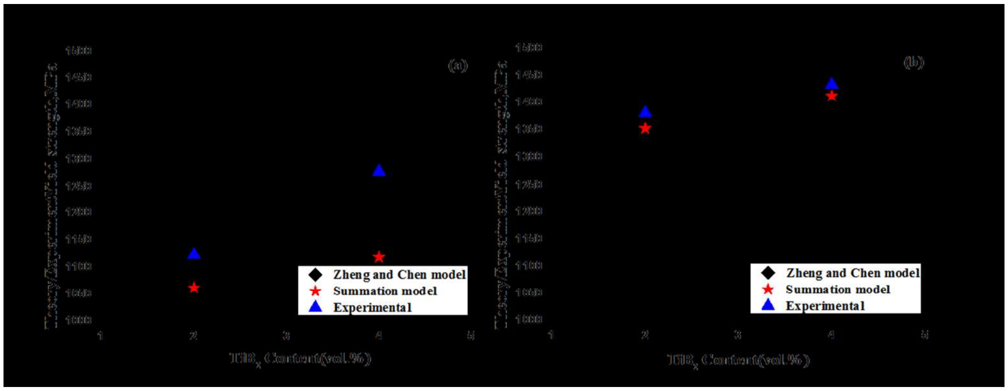

Figure 9. Comparative analysis between numerical models and experimental data sintered at 1000 ºC and (b) 1100 ºC

212x81mm (150 x 150 DPI)

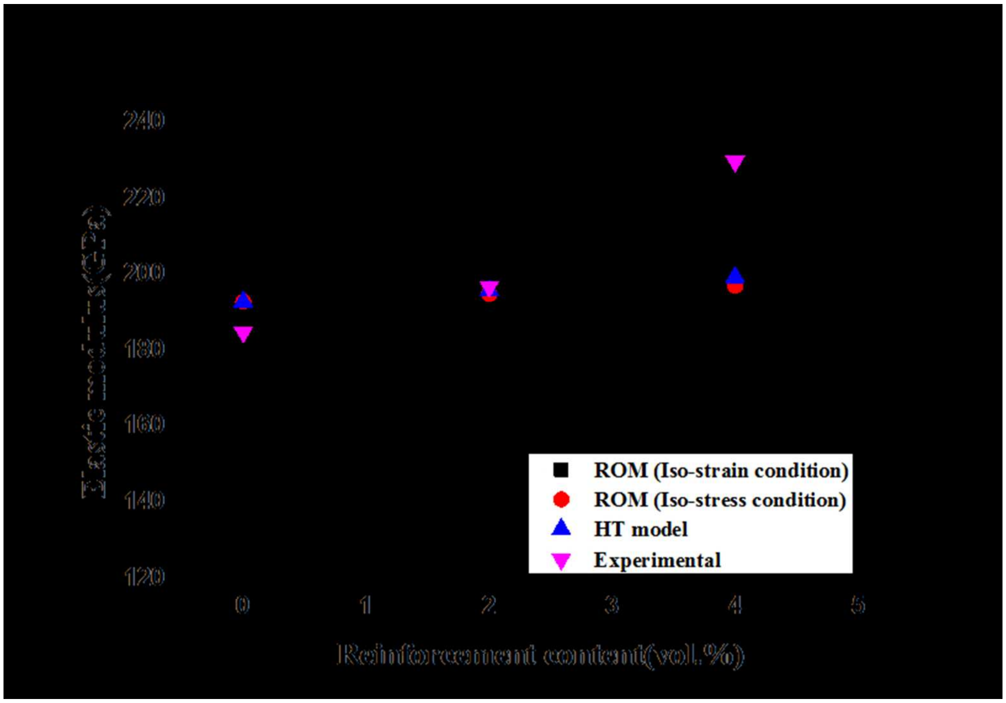

Figure 10. Comparison between experimental and predicted elastic modulus using HT model and ROM.

137x95mm (150 x 150 DPI)

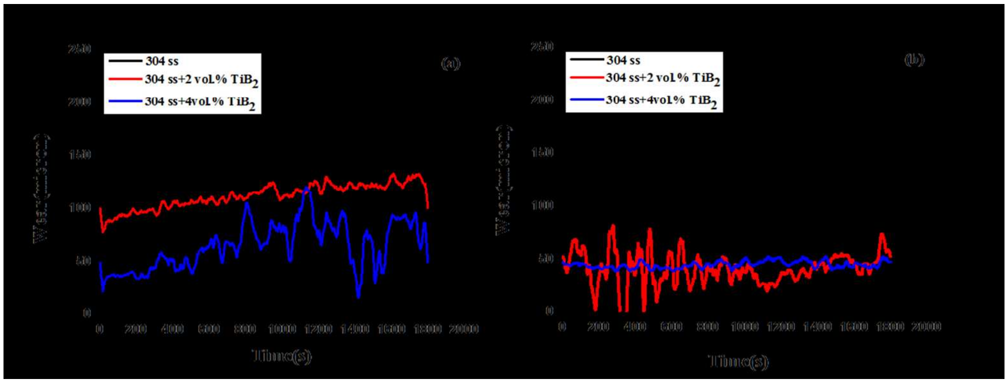

Figure 11. Variation of depth of wear with test time of the synthesized composites sintered at (a) 1000 ºC and (b) 1100 ºC.

215x80mm (150 x 150 DPI)

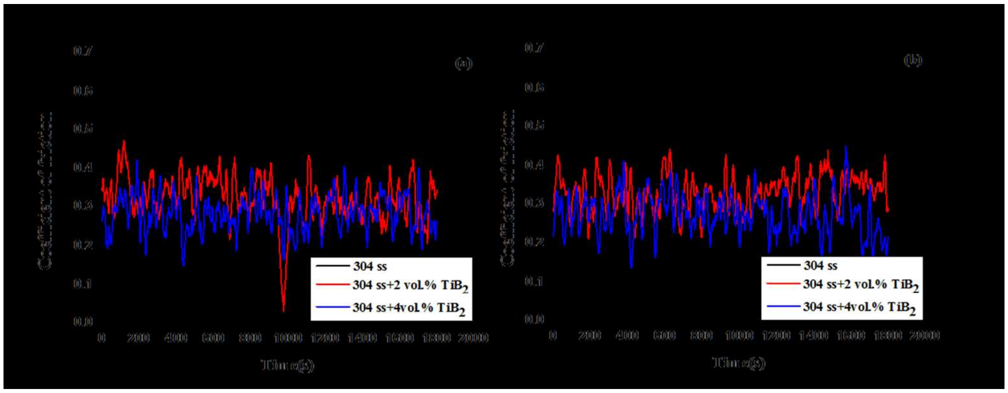

Figure 12. Variation of Coefficient of friction of the synthesized composites with test time sintered at (a) 1000 ºC and (b) 1100 ºC.

210x81mm (150 x 150 DPI)

Table 1. Composition of AISI 304 Stainless Steel powder (in wt.%)

Grade	C	Mn	Si	P	S	Cr	Mo	Ni	N
AISI304 SS	0.03	2.0	0.75	0.045	0.03	18.0	3.00	10.0	0.10

Table 2.

Material properties and parameters for calculating the improvement of the yield strength (Frost and Ashby 1982).

Properties	**Steel matrix**	**TiB_2 reinforcement**
Shear modulus(G_m),GPa	81	191
Burger vector(b), nm	0.258	-
Process temperature, K	1273,1373	1273,1373
Test temperature, K	298	298
Coefficient of thermal expansion (CTE), K^{-1}	$18x10^{-6}$	$8x10^{-6}$
Average particle size (d_p), µm		0.7-0.8